Few-Body Syst (2017) 58:139
DOI 10.1007/s00601-017-1299-x

Daniel Kikoła · Miguel García Echevarria · Cynthia Hadjidakis · Jean-Philippe Lansberg · Cédric Lorcé · Laure Massacrier · Catarina Quintans · Andrea Signori · Barbara Trzeciak

Feasibility Studies for Single Transverse-Spin Asymmetry Measurements at a Fixed-Target Experiment Using the LHC Proton and Lead Beams (AFTER@LHC)

Received: 6 February 2017 / Accepted: 10 April 2017 / Published online: 17 May 2017

Abstract The measurement of Single Transverse-Spin Asymmetries, A_N, for various quarkonium states and Drell–Yan lepton pairs can shed light on the orbital angular momentum of quarks and gluons, a fundamental ingredient of the proton-spin puzzle. The AFTER@LHC proposal combines a unique kinematic coverage and large luminosities thanks to the Large Hadron Collider beams to deliver precise measurements, complementary to the knowledge provided by collider experiments such as at RHIC. In this paper, we report on sensitivity studies for J/ψ, Υ and Drell–Yan A_N done using the performance of LHCb-like or ALICE-like detectors, combined with polarised gaseous hydrogen and helium-3 targets. In particular, such analyses will provide us with new insights and knowledge about transverse-momentum-dependent parton distribution functions for quarks and gluons and on twist-3 collinear matrix elements in the proton and the neutron.

Contents

This article belongs to the Topical Collection “New Observables in Quarkonium Production”.

D. Kikoła (✉)
Faculty of Physics, Warsaw University of Technology, Warsaw, Poland
E-mail: kikola@if.pw.edu.pl

M. G. Echevarria
FQA and ICCUB, Universitat de Barcelona, Martí i Franquès 1, 08028 Barcelona, Spain

C. Hadjidakis · J.-P. Lansberg · L. Massacrier
IPNO, CNRS-IN2P3, Univ. Paris-Sud, Université Paris-Saclay, 91406 Orsay Cedex, France

C. Lorcé
CPhT, Ecole Polytechnique, CNRS, Université Paris-Saclay, Palaiseau, France

C. Quintans
LIP, Lisbon, Portugal

A. Signori
Theory Center, Thomas Jefferson National Accelerator Facility, 12000 Jefferson Avenue, Newport News, VA 23606, USA

B. Trzeciak
Institute for Subatomic Physics, Utrecht University, Utrecht, The Netherlands

1 Introduction

1.1 Single Transverse-Spin Asymmetries: What for?

The spin is a fundamental quantity of a nucleon, yet its origins are largely unknown. It has been a topic of intense theoretical and experimental studies since the European Muon Collaboration reported that the spin of constituent quarks only accounts for a small fraction of the observed spin, $1/2$ [1]. Nowadays, it is accepted that both quarks and gluons as well as their relative motion, via the orbital angular momentum (OAM), contribute to the nucleon spin. For instance, in the case of a longitudinally polarised nucleon, i.e. with helicity $+\frac{1}{2}$, the spin is given by a sum rule

$$\frac{1}{2} = \frac{1}{2}\Delta\Sigma + \Delta G + \mathcal{L}_q + \mathcal{L}_g \,, \tag{1}$$

where $\frac{1}{2}\Delta\Sigma$ is the combined spin contribution of the quarks and the antiquarks, ΔG is the gluon spin, and $\mathcal{L}_{q,g}$ are the quark and gluon OAM contributions. Recent experimental data have shown that the spin distributions of quarks and antiquarks only account for about 25% of proton total longitudinal spin [2], and that of the gluons for about 20% for $x > 0.05$ [3], yet compatible with zero. The remaining proton spin therefore should arise from the relative dynamics of quarks and gluons, i.e. via $\mathcal{L}_q$ and $\mathcal{L}_g$. Understanding the parton transverse dynamics should then shed light on the origin of the proton spin.

The transverse-spin distributions give access to the aforementioned intrinsic properties of the proton constituents: their transverse and orbital-angular momenta. Contrary to the quark sector, very little is known about the gluon contributions via ΔG and $\mathcal{L}_g$ to the transverse spin. Only recently, COMPASS observed a non-zero asymmetry on the order of 20% (2σ away from zero) which hints at a non-zero value of $\mathcal{L}_g$ [4,5]. Indeed, whereas Single Transverse-Spin Asymmetries (STSAs), A_N, are not directly connected to $\mathcal{L}_{q,g}$, a non-zero A_N imposes that $\mathcal{L}_{q,g}$ is non-zero.

Such studies require gluon-sensitive observables. Naturally, quarkonium production can serve as such a tool, since the gluon fusion is the dominant contribution to these processes in high-energy hadron collisions (see [6–8] for RHIC energies). Thanks to many different experiments performed in the last decades (for reviews see [9–11]), measuring quarkonia via leptonic decays became a relatively straightforward task. The downside remains a lower production cross-section compared to light mesons, which calls for large integrated luminosities. Lastly, accessing transverse-spin physics research requires a polarised target. However, the interest in such studies [12] is growing.

At the moment, only the Relativistic Heavy Ion Collider (RHIC) at the Brookhaven National Laboratory provides polarised pp collisions at large enough energies for STSA measurements for quarkonia. Indeed, the PHENIX collabration [13] pioneered the studies of $p^\uparrow p \to J/\psi X$. The precision of the measurement is however very limited and did not allow to claim for a non-zero STSA, or to constrain $\mathcal{L}_g$. The COMPASS detector is probably the other existing experimental set-up where quarkonium STSA can be measured. Measurements of other quarkonium states are extremely important. First, J/ψ production involves a complicated pattern of feed downs and vector quarkonium production is not the easiest case to analyse theoretically. C-even quarkonia ($\chi_{c,b}$, η_c) which can be produced alone without recoiling gluons indeed offer some advantages. We refer to [14–17] for more details.

1.2 AFTER@LHC: Why?

AFTER@LHC is a proposal [18] for a fixed-target experiment using the LHC proton and heavy-ion beams at high and continuous luminosities, yet parasitic to the other LHC experiments. It bears on a particularly wide range of physics opportunities [16,19–52] thanks to the typical boost of the fixed-target mode between the center-of-mass (c.m.s.) and the laboratory frame converting forward detectors into backward ones, to relatively high luminosities and not too low c.m.s. energies, 115 GeV per nucleon with the 7 TeV proton beam and 72 GeV per nucleon with the 2.76 TeV lead beam. In this energy range, the cross section for quarkonium production is already high and gluon fusion dominates. Larger charmonium, bottomonium, D, B and Drell–Yan pair yields are expected compared to previous fixed-target experiments.

AFTER@LHC will also give access to the target-fragmentation region $x_F \to -1$, with detectors similar to the ALICE or LHCb ones, enabling the exploration of large momentum fractions in the target. Moreover, it is relatively easy to use a polarised gas target [53] in one of the existing LHC experiments keeping high integrated luminosities. Doing so, spin studies in the gluon sector via gluon-sensitive probes become more than possible with the investigation of spin correlations such as the Sivers effect [54–57] or the correlation between the gluon transverse momentum (denoted k_T thereafter) and the nucleon spin.

All this allows for measurements of gluon sensitive probes with an unprecedented quality in a region, large $x^\uparrow$, where theory calculations [36] predict that the effect (the observed spin-correlated azimuthal modulation of the produced particles) is the largest. We stress that the same observation obviously holds for open heavy flavour and Drell–Yan pairs.

The structure of the paper is as follows. In the next section, we recall some theoretical concepts related to spin studies with AFTER@LHC. Next, we present feasibility studies for STSAs and prospects for other spin-related measurements. The last section gathers our conclusions.

2 Theory

In order to measure the parton OAM, one should consider observables which are sensitive to both the parton transverse position and momentum. These are usually related to the Generalised Parton Distributions, accessible via exclusive processes. However, one can also indirectly obtain information on the orbital motion of partons via STSAs in hard-scattering processes, where one of

the colliding hadrons is transversely polarised (see e.g. [56,57] for recent reviews). These asymmetries are naturally connected to the transverse motion of partons inside hadrons [58].

The STSA, denoted by A_N, is the amplitude of the spin-correlated azimuthal modulation of the produced particles and it can be evaluated by studying the left-right asymmetry of the produced particles. Equivalently, the asymmetry may be quantified by measuring production cross sections for reactions with the target spin polarised upwards and downwards [59]:

$$A_N = \frac{1}{P}\frac{\sigma^{\uparrow} - \sigma^{\downarrow}}{\sigma^{\uparrow} + \sigma^{\downarrow}}, \tag{2}$$

where $\sigma^{\uparrow(\downarrow)}$ is the differential cross section (or yield) of particles produced with the target spin polarised upwards (downwards) with respect to the incoming beam direction, and P is the effective target polarisation. Studying A_N is of particular interest because leading-twist collinear perturbative QCD predicted it to be small ($A_N \propto m_q/p_T \sim O(10^{-4})$), while A_N was observed to be ∼10% or even larger at high x_F in polarised collisions over a broad range of energies [60–62]. For example, at Fermilab STSAs on the order of 10% were measured in hadronic polarised hyperon production [63,64] and pion production [61,65–67].

Since then, the study of spin asymmetries has rapidly evolved, both from the theoretical and experimental point of view (for detailed insights into spin physics and azimuthal asymmetries, see e.g. [68–78]). This triggered investigations of the hadron structure beyond the collinear parton model, and different mechanisms were proposed to account for spin asymmetries [70,71].

The first interpretation of STSAs relied on a collinear factorisation framework [79,80], involving interactions of gluons from the target remnants with the active partons in the initial and final states. This is accounted for by collinear twist-3 (CT3) matrix elements, the so-called Efremov–Teryaev–Qiu–Sterman (ETQS) matrix elements. Later, Sivers proposed an explanation [54,81] based on a correlation between the transverse momentum of the quark and the polarisation of the proton, introducing the quark transverse momentum dependent parton distribution function (TMD PDF) $f_{1T}^{\perp}(x, k_T^2)$ (the so-called Sivers function). The common feature of these two mechanisms is that an imaginary phase required for the non-vanishing asymmetry is generated by taking into account an additional gluon exchange between the active parton and the remnant of the transversely polarised hadron.

The CT3 formalism is valid for processes with only one characteristic hard scale, for instance the transverse momentum of a produced hadron, satisfying $p_{hT} \gg \Lambda_{\rm QCD}$, in a proton–proton collision. The TMD formalism [82–86], on the other hand, is suited for processes with two characteristic and well-separated scales (for example, in Drell–Yan process, the mass M and the transverse momentum p_T of the produced lepton pair, where $\Lambda_{\rm QCD} \lesssim p_T \ll M$).[1] When the two relevant scales become comparable, the TMD formalism can be then reduced to the CT3 one. In practice, this is realised in terms of an operator product expansion, since the Sivers TMD function can be matched onto the ETQS matrix elements at large transverse momenta. Thus, depending on the process, A_N should be addressed either using the CT3 formalism through 3-parton correlation functions, or the TMD formalism through the Sivers function.

One of the most important predictions, shared by both approaches, is the predictable, but non-universal, magnitude of this asymmetry in different processes. The experimental check of this feature is one of the milestones of the AFTER@LHC spin physics program.

2.1 Quark Sivers Effect

Drell–Yan (DY) lepton-pair production is a unique playground to understand the physics underlying the Sivers effect: it is theoretically very well understood and the quark Sivers function $f_{1T}^{\perp q}(x, k_T^2)$ enters the differential cross sections for DY and semi-inclusive deep inelastic scattering (SIDIS)[2] with opposite sign [89]:

$$f_{1T}^{\perp q}(x, k_T^2)\Big|_{\rm DY} = -f_{1T}^{\perp q}\left(x, k_T^2\right)\Big|_{\rm SIDIS}. \tag{3}$$

$f_{1T}^{\perp q}(x, k_T^2)$ accounts for the number density of unpolarised quarks carrying a longitudinal fraction x of the proton momentum and with transverse momentum k_T for a given transverse spin of the proton S_T. The verification of this "sign change" is the main physics case of the DY COMPASS run [90] and the experiments E1039 [91] and E1027 [92] at Fermilab. AFTER@LHC is a complementary facility to further investigate the quark Sivers effect by measuring DY STSAs [36,52] over a wide range of $x^{\uparrow}$ in a single set-up. With the high precision that AFTER@LHC will be able to achieve, it will clearly consolidate previous possible measurements. If the asymmetry turns out to be small and these experiments cannot get to a clear answer, AFTER@LHC could still confirm or falsify this sign-change prediction and put strict constraints on the Sivers effect for quarks.

In addition, given that this asymmetry can be framed as well within the CT3 approach when the transverse momentum of the produced lepton pair is comparable to its mass, AFTER@LHC will also generate very useful data to constrain the ETQS 3-parton correlation functions. The latter can also be determined by using direct γ production [93].

[1] See also e.g. [87,88] for what is known in the literature as the generalised parton model, which is an extension of the collinear perturbative QCD approach to incorporate the transverse dynamics of partons, and resembles the TMD formalism from a more phenomenological perspective.

[2] In SIDIS one of the leading hadrons is also detected, in addition to the lepton that is deflected.

2.2 Gluon Sivers Effect

The gluon Sivers function is more involved than its quark analogue: different processes probe different gluon Sivers functions, due to the inherent process dependence of this TMD function [94,95]. However all of them can be expressed in terms of only two independent functions [94,96], which will appear in different combinations depending on the process. AFTER@LHC will prove to be extremely useful in disentangling them and testing this generalised universality.

Drell–Yan lepton-pair production is the golden process to access the intrinsic transverse motion of quarks in a nucleon. However, there is no analogous process, which is at the same time experimentally clean and theoretically well-controlled, to probe the gluon content. One of the best tools at our disposal is the production of quarkonium states and open heavy-flavour mesons, a major strength of AFTER@LHC. They provide final states with a typical invariant mass ($M_{\mathcal{Q}}$) which is, on the one hand, small enough to be sensitive to the intrinsic transverse momenta of gluons (k_T), and on the other, large enough to realise the hierarchy of scales ($M_{\mathcal{Q}} \gg k_T$), and thus to allow for the TMD formalism to be applied without pollution from higher-twist effects. To this extent, production of C-even states can be fruitfully investigated [15,16,20,24,86,97].

The hadroproduction of η_c has already been measured by LHCb at high transverse momentum above $p_T = 6$ GeV [98], as well as non-prompt $\eta_c(2S)$ [99]. With an LHCb-like detector, STSAs for χ_c, χ_b and η_c are at reach, as demonstrated by studies of various χ_c states [100,101] in the busier collider environment down to p_T as low as 2 GeV/c. At lower energies, the reduced combinatorial background will give access to lower p_T. Moreover, with AFTER@LHC, the production of J/ψ, ψ' and Υ will also allow for accurate measurements of the gluon Sivers effect, as it is shown in the next Section.

The open heavy-flavour production also allows to investigate the process dependence of A_N (measuring charm quarks and anti-quarks separately) [102]. Moreover, it is a unique probe of C-parity odd twist-3 tri-gluon correlators [103,104], for which AFTER@LHC will obtain valuable information.

Finally, momentum imbalance observables also provide a very useful handle to probe the gluon Sivers function and its k_T dependence. $J/\psi + \gamma$ production is probably one of the cleanest from the theoretical point of view [105] along with di-J/ψ production.

3 Feasibility Studies for Quarkonium and DY A_N

3.1 Simulation Setup

We consider here two possible options for the realisation of AFTER@LHC with a polarised target: using the LHCb detector [106] or the ALICE detector [107]. LHCb is a multi-purpose, single arm detector with a precise microvertexing instrumentation, particle identification systems, electromagnetic and hadronic calorimeters. It has capabilities for an accurate primary and secondary vertex location determination, for a particle identification (including π, K, p, e and μ) with a good momentum resolution and a high rate data acquisition system. LHCb has already successfully run in the fixed-target mode using its luminosity monitor SMOG (System for Measuring the Overlap with Gas) [108] as a gas target. However, the data taking was done over limited periods of time and limited gas pressures. Additional feasibility studies are needed to address the possibility of installing a polarised gas target. The simulation setup we will use for a LHCb-like detector is described in detail in [35]. We therefore only outline here the most relevant information for Drell–Yan and J/ψ , $\Upsilon \to \mu^+\mu^-$ measurements, namely: the single muon tracking and the identification efficiency is ∼98% and the kinematic acceptance is $2 < \eta < 5$ and a p_T threshold is set at $p_T > 0.7\,\mathrm{GeV}/c$. However, for the studies presented in this paper, we used a more stringent cut of $p_T > 1.2\,\mathrm{GeV}/c$ which usefully reduces the uncorrelated background.

For ALICE, a target can in principle be placed, either at the nominal interaction point ($IP_Z = 0$), or upstream from the nominal one (for instance at 5 m, $IP_Z = -5$ m). The Muon Spectrometer would then provide a setup for di-muon pair measurements with a single track acceptance of $2.5 < \eta < 4$ for $IP_Z = 0$, and $3.2 < \eta < 4.2$ for $IP_Z = -5$ m. The Muon Forward Tracker (MFT) [109], which will be installed in the near future, will add tracking capabilities for muon measurements for $IP_Z = 0$. A typical single track p_T threshold for di-muon pair analysis with the ALICE Muon Arm is $p_T > 1\,\mathrm{GeV}/c$ [110]. In addition, the muon arm is equipped with an absorber, which reduces the uncorrelated background due to misidentified hadrons in such studies. Moreover, it is possible to install an additional vertexing instrumentation near the interaction point for $IP_Z = -5$ m. Such a vertex detector would improve the precision of Drell–Yan measurements by removing the background muons from light-hadron and charm/bottom-hadron decays. Indeed, for $IP_Z = -5$ m, the acceptance of the MFT does not match that of the spectrometer.

To quantify the STSA, we use the amplitude of the spin-correlated azimuthal modulation of the produced particles A_N. We consider the following approach to the A_N measurement with di-muon pairs. For the statistical precision evaluation, we assume that the yields $\sigma^\uparrow, \sigma^\downarrow$ are separately measured with a standard invariant mass approach used in high energy experiments for quarkonium studies. We construct an invariant mass spectrum of all di-muon pairs (often called *foreground*) which contains both signal of interest (J/ψ, Υ, DY) and random pairs (combinatorial background, B). The background yield B is evaluated with a like sign technique: by taking a sum of mass distributions for $\mu^+\mu^+$ and $\mu^-\mu^-$, or a geometric mean of like-sign pair yields ($2\sqrt{N_{\mu^+\mu^+}N_{\mu^-\mu^-}}$). Finally, we subtract the background from the foreground to get the signal yield for a given target polarisation in a given kinematical domain. PHENIX used such an approach in J/ψ A_N measurement [13] and their study confirmed that the like-sign pairs represent well the yield and polarisation of the uncorrelated background. The statistical uncertainty δ_σ on the $\sigma^\uparrow, \sigma^\downarrow$ is thus given by $\delta_\sigma = \sqrt{\sigma + 2B}$, and the statistical uncertainty on A_N reads $\delta_{A_N} = \frac{2}{P(\sigma^\downarrow + \sigma^\uparrow)^2}\sqrt{(\delta_{\sigma^\uparrow}\sigma^\downarrow)^2 + (\delta_{\sigma^\downarrow}\sigma^\uparrow)^2}$. The factor $2B$ in δ_σ definition accounts for the statistical uncertainty from the combinatorial background subtraction in the A_N evaluation. This approach assumes that the luminosities for each polarisation configuration are the same; if not, then the $\sigma^\uparrow, \sigma^\downarrow$ need to be corrected for the relative luminosity differences. Similarly, we consider here that the systematic effects (like the detector acceptance) are the same for $\sigma^\uparrow$ and $\sigma^\downarrow$, and will cancel out in the ratio. If they are not, this should be accounted for. We also assume that a microvertexing detector will allow us to remove the correlated background from charm and bottom hadron decays. Thanks to the boost effect, their decay vertex is well separated from the primary collision point and $c \to \mu$ and

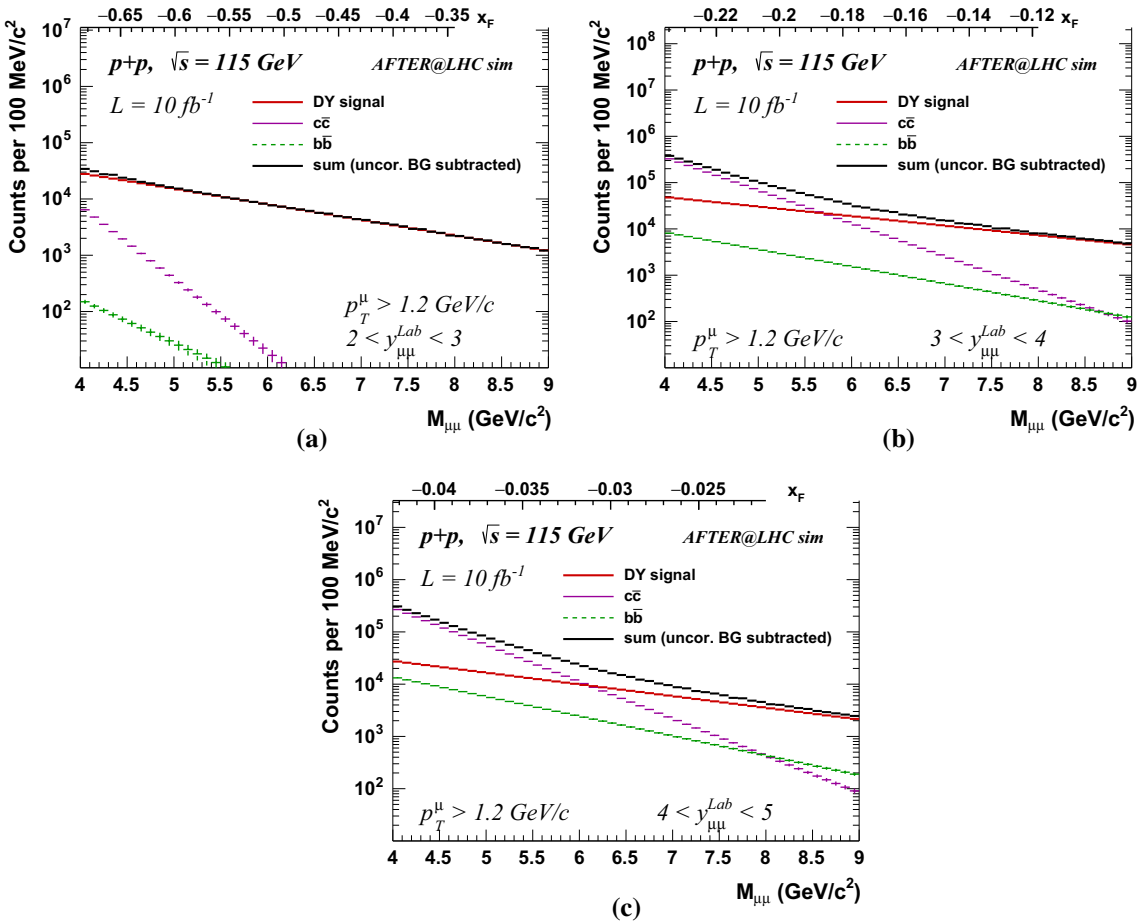

Fig. 1 Invariant mass distribution of the correlated $\mu^+\mu^-$ pairs originating from Drell–Yan, $c\bar{c}$ and $b\bar{b}$ production for a LHCb-like detector. The uncorrelated background is estimated with the like-sign method and then subtracted from the overall simulated $\mu^+\mu^-$ mass spectrum. **a** $2 < y^{\text{Lab}}_{\mu^+\mu^-} < 3$ $(-2.8 < y^{\text{c.m.s}}_{\mu^+\mu^-} < -1.8)$, **b** $3 < y^{\text{Lab}}_{\mu^+\mu^-} < 4$ $(-1.8 < y^{\text{c.m.s}}_{\mu^+\mu^-} < -0.8)$, **c** $4 < y^{\text{Lab}}_{\mu^+\mu^-} < 5$ $(-0.8 < y^{\text{c.m.s}}_{\mu^+\mu^-} < 0.2)$

$b \to \mu$ could be identified by measuring the track offset from the primary vertex. If the event-by-event tagging of $c \to \mu$ and $b \to \mu$ is not possible due to a finite resolution, these muons can be identified on a statistical basis, as it was done by the NA60 experiment [111]. Then the charm and bottom contributions could be subtracted from the invariant mass distribution separately for interactions with the target spin polarised upwards and downwards, and thus removed from the A_N measurement.

3.2 Yields and Kinematical Range for the A_N Measurements with a LHCb-Like Detector

The statistical precision of quarkonium and Drell–Yan measurements with a LHCb-like detector was obtained with realistic $p + p$ simulations at $\sqrt{s} = 115$ GeV of correlated and uncorrelated background [35]. First, the invariant mass spectrum of all $\mu^+\mu^-$ pairs (M_{All}) is computed, which includes the signal (correlated pairs), the correlated background (mainly muon pairs from semileptonic decays of charmed and bottom hadrons) and the so-called combinatorial background (uncorrelated, randomly combined muon pairs in the analysis). We applied a single-muon p_T threshold of $p_T > 1.2\,\text{GeV}/c$ to reduce the background. We estimated the invariant-mass distribution of the uncorrelated background with the like-sign technique and then subtracted it from M_{All} to account for the statistical uncertainty owing to the background fluctuations. Figure 1 shows examples of the resulting invariant-mass distributions of the correlated $\mu^+\mu^-$ pairs for three rapidity bins: $2 < y^{\text{Lab}}_{\mu^+\mu^-} < 3$, $3 < y^{\text{Lab}}_{\mu^+\mu^-} < 4$ and $4 < y^{\text{Lab}}_{\mu^+\mu^-} < 5$ for a LHCb-like detector. Because of the Lorentz boost of 4.8 units of rapidity in the case of the proton beam in AFTER@LHC these rapidity bins correspond to the c.m.s. ranges of $-2.8 < y^{\text{c.m.s}}_{\mu^+\mu^-} < -1.8$, $-1.8 < y^{\text{c.m.s}}_{\mu^+\mu^-} < -0.8$ and $-0.8 < y^{\text{c.m.s}}_{\mu^+\mu^-} < 0.2$, respectively. In addition to the Drell–Yan and quarkonium studies, the double-J/ψ production is of interest because it gives access to the k_T evolution of the gluon Sivers function. The double J/ψ rates are calculated within LHCb-like acceptance [33] assuming a negligible background (which is an acceptable approximation given the background level

Table 1 J/ψ, Υ and double J/ψ yields expected with a LHCb-like detector per LHC year with a 7 TeV proton beam on a proton target assuming $\mathcal{L}_{\rm int} = 10\ {\rm fb}^{-1}$

	$2 < y^{\rm Lab}_{\mu^+\mu^-} < 3$ $(-2.8 < y^{\rm c.m.s}_{\mu^+\mu^-} < -1.8)$	$3 < y^{\rm Lab}_{\mu^+\mu^-} < 4$ $(-1.8 < y^{\rm c.m.s}_{\mu^+\mu^-} < -0.8)$	$4 < y^{\rm Lab}_{\mu^+\mu^-} < 5$ $(-0.8 < y^{\rm c.m.s}_{\mu^+\mu^-} < 0.2)$
J/ψ	1.69×10^7	1.04×10^8	1.01×10^8
	$3 < y^{\rm Lab}_{\mu^+\mu^-} < 4$ $(-1.8 < y^{\rm c.m.s}_{\mu^+\mu^-} < -0.8)$	$4 < y^{\rm Lab}_{\mu^+\mu^-} < 5$ $(0.8 < y^{\rm c.m.s.}_{\mu^+\mu^-} < 0.2)$	$3 < y^{\rm Lab}_{\mu^+\mu^-} < 5$ $(-1.8 < y^{\rm c.m.s}_{\mu^+\mu^-} < 0.2)$
$\Upsilon(1S)$	4.85×10^4	8.85×10^4	1.37×10^5
$\Upsilon(2S)$	9.57×10^3	1.85×10^4	2.81×10^4
$\Upsilon(3S)$	4.35×10^3	8.77×10^3	1.31×10^4
	$2 < y^{\rm Lab} < 5$ $(-2.8 < y^{\rm c.m.s}_{\mu^+\mu^-} < 0.2)$		
Double J/ψ	780		

Table 2 Drell–Yan yields for $4 < M_{\mu^+\mu^-} < 9\,{\rm GeV}/c^2$ expected with a LHCb-like detector per LHC year with a 7 TeV proton beam on a proton target assuming $\mathcal{L}_{\rm int} = 10\ {\rm fb}^{-1}$

	$2 < y^{\rm Lab}_{\mu^+\mu^-} < 3$ $(-2.8 < y^{\rm c.m.s}_{\mu^+\mu^-} < -1.8)$	$3 < y^{\rm Lab}_{\mu^+\mu^-} < 4$ $(-1.8 < y^{\rm c.m.s}_{\mu^+\mu^-} < -0.8)$	$4 < y^{\rm Lab}_{\mu^+\mu^-} < 5$ $(-0.8 < y^{\rm c.m.s}_{\mu^+\mu^-} < 0.2)$
Drell–Yan yield	4.32×10^5	9.32×10^5	4.98×10^5
Like-sign pairs yield	5.84×10^5	1.86×10^7	4.53×10^6
Signal-to-background ratio	0.74	0.05	0.11

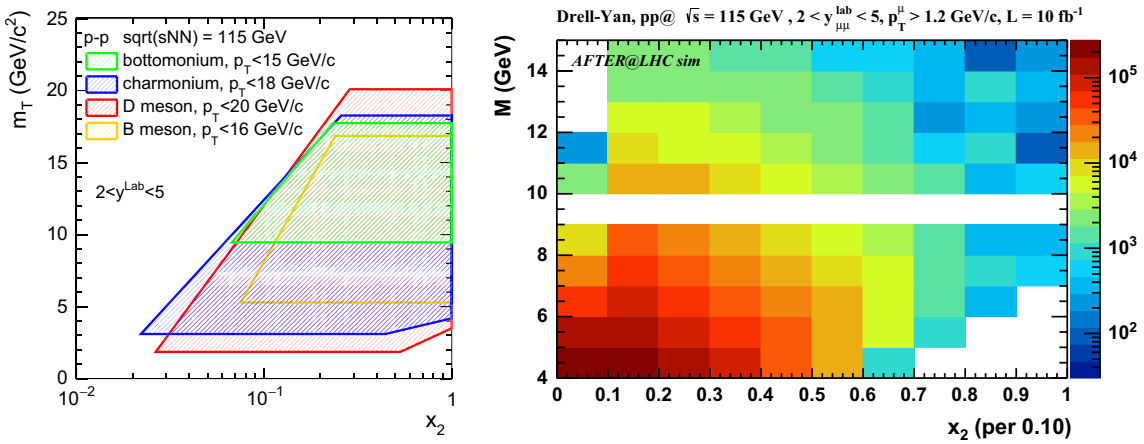

Fig. 2 *Left panel* the range in the transverse mass m_T versus parton momentum fraction x_2 accessible in AFTER@LHC in $p+p$ collisions at $\sqrt{sNN} = 115$ GeV with J/ψ, Υ, B- and D-meson measurements. We assume that the maximum p_T reachable in AFTER@LHC is ~15 GeV/c for bottomonium, ~16 GeV/c for B-meson, ~18 GeV/c for charmonium and ~20 GeV/c in the case of D-meson. *Right panel* the x_2 versus Drell–Yan mass coverage. [Both are for a LHCb-like detector]

observed for single J/ψ [35]). Tables 1 and 2 summarises the expected J/ψ, double J/ψ, $\Upsilon$and Drell–Yan yields for a single data taking year for $\mathcal{L}_{\rm int} = 10\ {\rm fb}^{-1}$.

Such an experimental set-up offers a unique kinematic coverage, which allows one to probe a wide range of the momentum fraction x_2. Figure 2 (left panel) shows the range in the transverse mass m_T versus x_2 that is available with the J/ψ, Υ and B and D-meson measurements.[3] Since these are gluon-sensitive probes, they give an unprecedented access to the gluon dynamics over a broad range of $0.02 < x_2 < 1$. Figure 2 (right panel) shows the corresponding kinematic coverage (mass vs. x_2) for the Drell–Yan pairs with the yield information. Any cell in colour contains at least 30 DY events.

[3] The momentum fractions of the partons x_2 is computed with a $2 \rightarrow 2$ kinematics [9] taking following approximation: $x_2 \approx 2m_T e^{-y}/\sqrt{s}$ for D, B mesons, and $x_2 \approx (m_T + p_T)e^{-y}/\sqrt{s}$ for quarkonium, with $m_T^2 = m^2 + p_T^2$, which corresponds to x_1 and x_2 minimising their product (threshold).

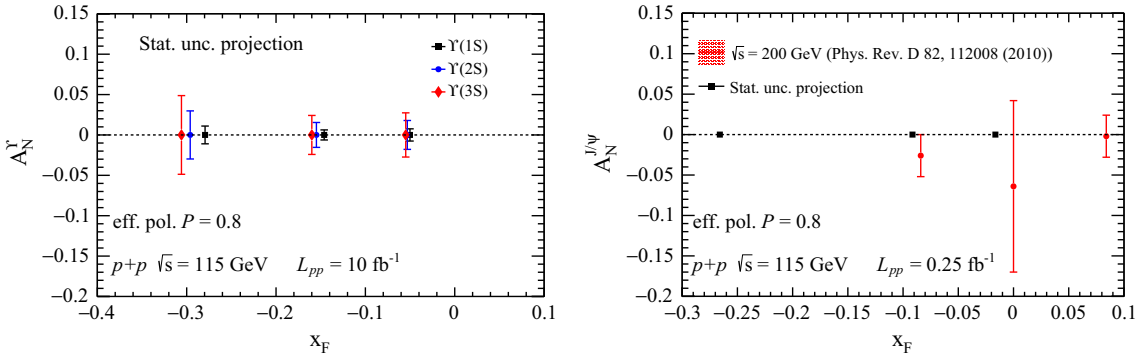

Fig. 3 Projections for Υ (*left panel*) and J/ψ (*right panel*) A_N as a function of x_F for AFTER@LHC with a LHCb-like detector. For the J/ψ case, these are compared to existing data from PHENIX [13] in *red*

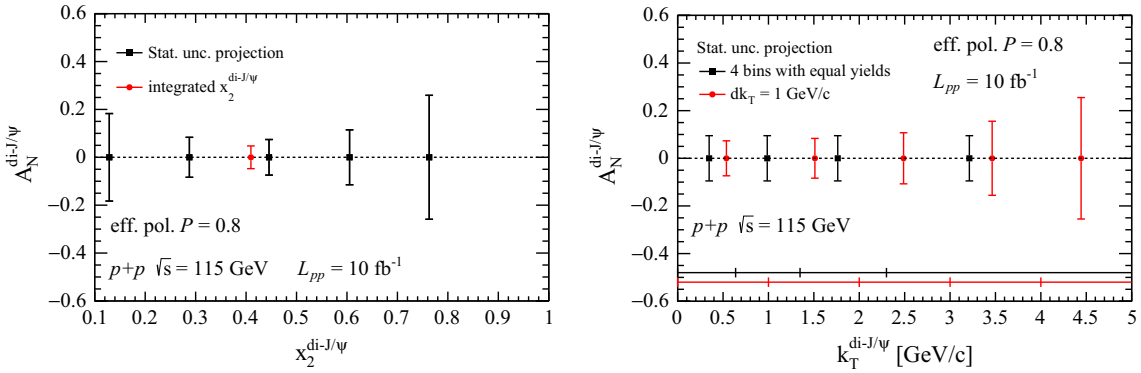

Fig. 4 Statistical projections for di-J/ψ A_N as a function of x_2 and the pair p_T with a LHCb-like detector. The *lines* at the *bottom of right hand side panel* denote width of the p_T bins used for the calculations

3.3 A_N in $p + p^{\uparrow}$ Collisions

Inspired from the performance of the polarised gas HERMES target [53] (which successfully operated for many years with an effective average transverse polarisation $P \sim 80\%$), we used $P = 80\%$ in the following statistical precision projections.

Figure 3 shows our precision projections for J/ψ and Υ A_N as a function of x_F. The statistical power of this measurement reflects the major strength of AFTER@LHC, namely an ideal acceptance with conventional detectors and the large production rates for quarkonium states expected for a single year of data taking (10^6 Υ and 10^9 J/ψ). Such a study will only be limited by the systematic uncertainties, which cancel out to a large extent in A_N. Even for a fraction of the expected luminosity ($\mathcal{L}_{\text{int}} = 1\ \text{fb}^{-1}$), $A_N^{J/\psi}$ can be measured with a per-mil precision. Moreover, the $A_N^{\Upsilon(nS)}$ is a unique observable, which is virtually inaccessible elsewhere and which can be measured with a few per cent accuracy with AFTER@LHC. This level of data quality will allow one to study the size of the asymmetry, its shape and the x_F dependence of quarkonium A_N. Furthermore, AFTER@LHC aims at measurements of A_N for nearly all quarkonium states, including C-even $\chi_{c,b}$ and η_c, and their associated production. These processes are sensitive to the gluon content of the colliding hadrons which can then be measured with an outstanding precision.

Associated-production channels [14,20,24,41,105,112,113] are fundamental tools to access the Gluon Sivers effect, and also probing the gluon TMD sector and their evolution [86,114]. A few different processes are potentially interesting in this context, for instance $J/\psi - J/\psi$, $J/\psi - \gamma$, $\gamma - \gamma$, $\Upsilon - \gamma$. The $J/\psi - J/\psi$ production seems to be the most practical one since the yields are not too small [33] and the measurement is relatively straightforward (compared, for instance, to direct γ studies). Figure 4 shows the A_N for double J/ψ production as a function of the pair x_2 and the pair k_T. We consider two scenarios for the analysis of A_N as a function of k_T: one with a fixed k_T bin width of 1 GeV/c ($dk_T = 1\,\text{GeV}/c$, red points) and four bins with equal yields. Here, we model the k_T dependence as a Gaussian distribution with the width $\sigma = 2\,\text{GeV}/c$. The x_2-integrated A_N will allow for the determination of the STSA with a few percent precision and the $A_N(k_T)$ gives access—for the first time—to the k_T dependence of the gluon Sivers TMD up to $k_T \approx 4\,\text{GeV}/c$.

As we mentioned in the previous section, Drell–Yan production is a unique probe of the Sivers effect for the quarks. It is a subject of lively interest with many existing or planned experiments (COMPASS, STAR, E1039). Table 3 shows a compilation of the relevant parameters of future or planned polarised DY experiments. AFTER@LHC is capable of measuring the Drell–Yan A_N in a broad kinematic range with exceptional precision.

Figure 5 shows the statistical accuracy expected with a single data-taking year using a LHCb-like detector, for the Drell–Yan pairs satisfying $4 < M_{\mu^+\mu^-} < 9\,\text{GeV}/c^2$. The level of uncorrelated background drives the statistical uncertainties of this

Table 3 Compilation inspired from [18,57] of the relevant parameters for the future or planned polarised DY experiments. The effective polarisation ($\mathcal{P}_{\text{eff}}$) is a beam polarisation (where relevant) or an average polarisation times a (possible) dilution factor (for a gas target, similar to the one developed for HERMES [53,115,116]) or a target polarisation times a dilution factor (for the NH_3 target used by COMPASS and E1039). For AFTER@LHC the numbers correspond to a gas target. $\mathcal{F}$ is the (instantaneous) spin figure of merit of the target defined as $\mathcal{F} = \mathcal{P}_{\text{eff}}^2 \times \mathcal{L}$, with $\mathcal{L}$ being the instantaneous luminosity

Experiment	Particles	Beam energy (GeV)	$\sqrt{s}$ (GeV)	$x^{\uparrow}$	$\mathcal{L}$ (cm^{-2}s^{-1})	$\mathcal{P}_{\text{eff}}$ (%)	$\mathcal{F}$ (cm^{-2}s^{-1})
AFTER@LHCb	$p + p^{\uparrow}$	7000	115	$0.05 \div 0.95$	1×10^{33}	80	6.4×10^{32}
AFTER@LHCb	$p + {}^3\text{He}^{\uparrow}$	7000	115	$0.05 \div 0.95$	2.5×10^{32}	23	1.4×10^{31}
AFTER@ALICE$_{\mu}$	$p + p^{\uparrow}$	7000	115	$0.1 \div 0.3$	2.5×10^{31}	80	1.6×10^{31}
COMPASS (CERN)	$\pi^- + p^{\uparrow}$	190	19	$0.05 \div 0.55$	2×10^{33}	18	6.5×10^{31}
PHENIX/STAR (RHIC)	$p^{\uparrow} + p^{\uparrow}$	Collider	510	$0.05 \div 0.1$	2×10^{32}	50	5.0×10^{31}
E1039 (FNAL)	$p + p^{\uparrow}$	120	15	$0.1 \div 0.45$	4×10^{35}	15	9.0×10^{33}
E1027 (FNAL)	$p^{\uparrow} + p$	120	15	$0.35 \div 0.9$	2×10^{35}	60	7.2×10^{34}
NICA (JINR)	$p^{\uparrow} + p$	Collider	26	$0.1 \div 0.8$	1×10^{32}	70	4.9×10^{31}
fsPHENIX (RHIC)	$p^{\uparrow} + p^{\uparrow}$	Collider	200	$0.1 \div 0.5$	8×10^{31}	60	2.9×10^{31}
fsPHENIX (RHIC)	$p^{\uparrow} + p^{\uparrow}$	Collider	510	$0.05 \div 0.6$	6×10^{32}	50	1.5×10^{32}
PANDA (GSI)	$\bar{p} + p^{\uparrow}$	15	5.5	$0.2 \div 0.4$	2×10^{32}	20	8.0×10^{30}

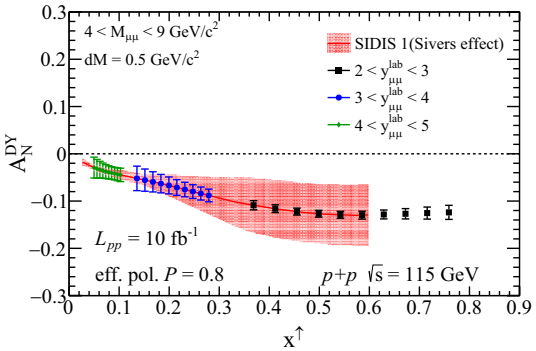

Fig. 5 Statistical projections for the Drell–Yan A_N measurement as a function of $x^{\uparrow}$ with a LHCb-like detector. Note that the range in $x^{\uparrow}$ is limited by the bin sizes in y and M. We have checked that measurements can probably be done with an accuracy of 5% up to $x^{\uparrow} \simeq 0.95$ as expected from Fig. 2

measurement. We estimated the background with the robust and commonly used like-sign technique, then we subtracted it from the $M_{\mu^+\mu^-}$ distribution. As explained above, we also assumed that the microvertexing detector allow one to remove the correlated background from charm and bottom pair decays. The AFTER@LHC projections are compared to a theory evaluation [36]. This theory prediction based on SIDIS currently exhibit uncertainties much larger than our projected uncertainties, as shown by this example. By delivering high-quality data over a wide kinematic range, AFTER@LHC will thus probe the $x^{\uparrow}$ dependence of the A_N^{DY} and constrain model calculations.

Since the statistical precision of A_N^{DY} strongly depends on the level of uncorrelated background, such a study can be carried out with lower integrated luminosity if the background is suppressed. The ALICE forward muon arm may provide a set-up with a lower background than a LHCb-like detector since the absorber in front of its muon detector significantly reduces the uncorrelated background. Such an effect is however difficult to simulate precisely. Moreover, the available integrated luminosity is limited by the ALICE data taking rate capabilities. An integrated luminosity of 0.25 fb^{-1} can be expected at best for a single year of data taking.

To check to which extent A_N^{DY} can be studied with ALICE and if this deserves further in-depth investigations, we estimated the signal and background yields as follows. First, we assumed that the number of uncorrelated pairs in the DY and charmonium measurements is proportional to the number of charged particles squared, N_{ch}^2. To take into account the track reconstruction efficiency and the background suppression by the ALICE absorber, we referred to ALICE measurements of the di-muon pairs at forward rapidities in pp collisions at 8 TeV [110]. Since Drell–Yan pairs were not measured by ALICE yet, we turned to $J/\psi \rightarrow \mu^+\mu^+$ measurements. We calculated the number of uncorrelated pairs N_{un} under the J/ψ peak and the J/ψ yield and we normalised them by the luminosity. Then, we used the scaling of charged track density with the collision energy $dN_{ch}/d\eta|_{\eta\sim 0} = 0.725(\sqrt{s})^{0.23}$ [117] to scale down the N_{un} to the level expected at $\sqrt{s} = 115$ GeV. Next, we used the energy dependence of the J/ψ cross section as calculated in the FONLL (Fixed Order plus Next-to-Leading Logarithms) framework to scale the J/ψ yield to the value expected at 115 GeV –admittedly this is another approximation. We neglected the change of the shape of $dN_{ch}/d\eta$ and $d\sigma^{J/\psi}/dy$ distributions with $\sqrt{s}$ for these first estimates. Finally, we assumed that the reconstruction efficiency for J/ψ and DY pairs was similar and the ratio of observed DY to J/ψ pairs would be the same in ALICE and LHCb. We thus used the correlated di-muon spectrum simulated for LHCb-like detector for $3 < y^{\text{Lab}}_{\mu^+\mu^-} < 4$ and scale it to match the

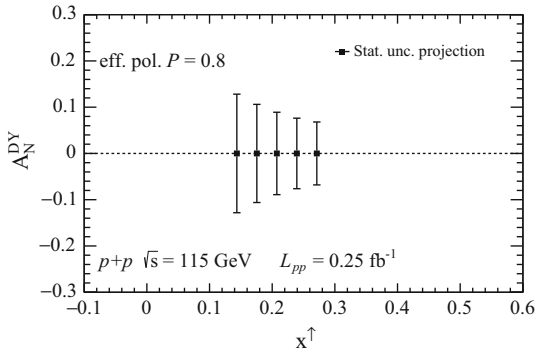

Fig. 6 Fast statistical projections for Drell–Yan A_N as a function of $x^{\uparrow}$ with a ALICE-like detector. See text for details

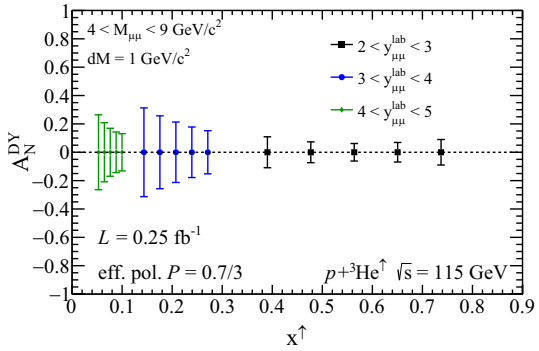

Fig. 7 Statistical projections for Drell–Yan A_N as a function of $x^{\uparrow}$ in $p+^3\mathrm{He}^{\uparrow}$ collisions at $\sqrt{s} = 115$ GeV

J/ψ yield in the simulation to that expected in ALICE at 115 GeV. Similarly, we normalised the uncorrelated background under the J/ψ peak in the simulations to the N_{un} estimated for ALICE in a fixed target mode. As a results, we obtained distributions of DY, $c\bar{c} \to \mu^+\mu^-$, $b\bar{b} \to \mu^+\mu^-$ and uncorrelated background pairs expected in the measurements using the ALICE muon arm.

Note that we implicitly assumed the target location to be at $z = 0$, which is not completely coherent with the location of a polarised target. We nevertheless believe this to be sufficient for such a prospective study. Figure 6 shows the projections for A_N measured with the ALICE-like acceptance of $3 < y^{\mathrm{Lab}}_{\mu^+\mu^-} < 4$. The uncertainties are sizeable but there is room for improvement if tracking and vertex detectors before the absorber are used to reject muons from π, K meson and beauty and charm hadrons decays.

3.4 Accessing the Quark Sivers Function in a Polarised Neutron: $p+^3\mathrm{He}^{\uparrow}$ Collisions

AFTER@LHC with a gas target offers a unique opportunity for studies of STSA in polarised $p+^3\mathrm{He}^{\uparrow}$ collisions. Such reactions give access to polarised neutrons and thus to the Sivers functions in a neutron which can shed some light on its isospin dependence. Figures 7 and 8 show the statistical-uncertainty predictions for DY and quarkonium A_N measurements. In the case of $^3\mathrm{He}^{\uparrow}$, a polarisation of P = 70% can be achieved [115,116]. However, the effective polarisation, $\mathcal{P}_{\mathrm{eff}}$, is diluted by a factor of 3 since only the neutron is polarised in the $^3\mathrm{He}^{\uparrow}$. In addition, the combinatorial background is proportional to the number of binary nucleon-nucleon collisions N_{coll}, thus the background increases by a factor $N_{coll} \approx \sqrt{3}$. An additional isospin factor of 9/6 for DY studies is included. The available integrated luminosity of 2.5 fb^{-1} will allow for an exploratory measurement for DY production and precision study for J/ψ A_N.

4 Conclusions

We have presented prospects and sensitivity studies for measurements of the quarkonia and Drell–Yan single transverse spin asymmetry which could be achieved with a fixed-target experiment at the LHC, AFTER@LHC, with a polarised gas target. Owing to its orginal acceptance, high target polarisation and large luminosities, AFTER@LHC can deliver a set of unparalleled, high-quality data that will allow for in-depth studies of the gluon and quark Sivers functions and of the 3-parton collinear twist-3 correlators.

The A_N for J/ψ, Υ, C-even quarkonium states and various associated-production channels can be measured with unprecedented precision. The latter will give access for the first time to the transverse momentum depedence of the gluon Sivers effect.

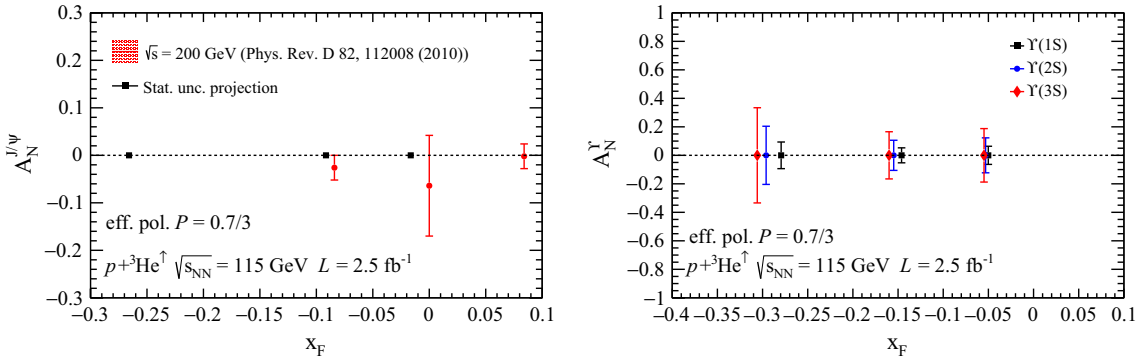

Fig. 8 Statistical projections for J/ψ and Υ A_N as a function of x_F in $p+^3\mathrm{He}^\uparrow$ collisions at $\sqrt{s} = 115$ GeV, compared to existing PHENIX data with polarised protons [13]

Such studies, along with those of the STSAs for open charm and beauty, make AFTER@LHC the best place to advance –in a close future– our knowledge of gluon and quark dynamics in a nucleon and of how they bind together to produce its observed spin 1/2.

Acknowledgements This research was supported in part by the French P2IO Excellence Laboratory, the French CNRS via the grants FCPPL-Quarkonium4AFTER & TMD@NLO. AS acknowledges support from U.S. Department of Energy contract DE-AC05-06OR23177, under which Jefferson Science Associates, LLC, manages and operates Jefferson Lab. MGE is supported by the Spanish Ministry of Economy and Competitiveness under the *Juan de la Cierva* program and grant FPA2013-46570-C2-1-P.

References

1. European Muon Collaboration, J. Ashman et al., A Measurement of the Spin Asymmetry and Determination of the Structure Function g(1) in Deep Inelastic Muon-Proton Scattering, Phys. Lett. **B206**, 364 (1988)
2. D. de Florian, R. Sassot, M. Stratmann, W. Vogelsang, Global analysis of helicity parton densities and their uncertainties. Phys. Rev. Lett. **101**, 072001 (2008). arXiv:0804.0422 [hep-ph]
3. STAR Collaboration, L. Adamczyk et al., Precision measurement of the longitudinal double-spin asymmetry for inclusive jet production in polarized proton collisions at $\sqrt{s} = 200$ GeV, Phys. Rev. Lett. **115**(9), 092002 (2015). arXiv:1405.5134 [hep-ex]
4. COMPASS Collaboration, K. Kurek, A. Szabelski, The Gluon Contribution to the Sivers Effect COMPASS results, J. Phys. Conf. Ser. **678**(1), 012055 (2016)
5. C. Adolph et al., First measurement of the Sivers asymmetry for gluons from SIDIS data. arXiv:1701.02453 [hep-ex]
6. Y. Feng, J.-P. Lansberg, J.-X. Wang, Energy dependence of direct-quarkonium production in pp collisions from fixed-target to LHC energies: complete one-loop analysis. Eur. Phys. J. C **75**(7), 313 (2015). arXiv:1504.00317 [hep-ph]
7. S.J. Brodsky, J.-P. Lansberg, Heavy-quarkonium production in high energy proton–proton collisions at RHIC. Phys. Rev. D **81**, 051502 (2010). arXiv:0908.0754 [hep-ph]
8. J.P. Lansberg, QCD corrections to J/psi polarisation in pp collisions at RHIC. Phys. Lett. B **695**, 149–156 (2011). arXiv:1003.4319 [hep-ph]
9. A. Andronic et al., Heavy-flavour and quarkonium production in the LHC era: from proton-proton to heavy-ion collisions, Eur. Phys. J. **C76**(3), 107 (2016). arXiv:1506.03981 [nucl-ex]
10. N. Brambilla et al., Heavy quarkonium: progress, puzzles, and opportunities. Eur. Phys. J. C **71**, 1534 (2011). arXiv:1010.5827 [hep-ph]
11. J. P. Lansberg, J/ψ, ψ' and Υ production at hadron colliders: a Review, Int. J. Mod. Phys. **A21**, 3857–3916 (2006). arXiv:hep-ph/0602091 [hep-ph]
12. R. M. Godbole, A. Kaushik, A. Misra, V. Rawoot, B. Sonawane, Transverse single spin asymmetry in $p + p^\uparrow \to J/\psi + X$. arXiv:1703.01991 [hep-ph]
13. PHENIX Collaboration, A. Adare et al., Measurement of transverse single-spin asymmetries for J/ψ production in polarized $p + p$ collisions at $\sqrt{s} = 200$ GeV, Phys. Rev. **D82**, 112008 (2010). arXiv:1009.4864 [hep-ex]. [Erratum: Phys. Rev.D86,099904(2012)]
14. D. Boer, Gluon TMDs in quarkonium production. Few Body Syst. **58**(2), 32 (2017). arXiv:1611.06089 [hep-ph]
15. A. Schafer, J. Zhou, Transverse single spin asymmetry in hadronic $\eta_{c,b}$ production. Phys. Rev. D **88**(1), 014008 (2013). arXiv:1302.4600 [hep-ph]
16. D. Boer, C. Pisano, Polarized gluon studies with charmonium and bottomonium at LHCb and AFTER. Phys. Rev. D **86**, 094007 (2012). arXiv:1208.3642 [hep-ph]

17. F. Yuan, Heavy quarkonium production in single transverse polarized high energy scattering. Phys. Rev. D **78**, 014024 (2008). arXiv:0801.4357 [hep-ph]
18. S.J. Brodsky, F. Fleuret, C. Hadjidakis, J.P. Lansberg, Physics opportunities of a fixed-target experiment using the LHC beams. Phys. Rep. **522**, 239–255 (2013). arXiv:1202.6585 [hep-ph]
19. S. Koshkarev, S. Groote, Double quarkonium production at high Feynman-x. Nucl. Phys. B **915**, 384–391 (2017). arXiv:1611.08149 [hep-ph]
20. A. Signori, *Flavor and Evolution Effects in TMD Phenomenology*. Ph.D. thesis, Vrije U., Amsterdam, 2016. http://inspirehep.net/record/1493030/files/Thesis-2016-Signori.pdf
21. S. Koshkarev, Production of the doubly heavy baryons, B_c meson and the Tetra-c-quark at the Fixed-target Experiment at the LHC with double intrinsic heavy approach Acta Physica Polonica B **48**(2), 163 (2017)
22. J. P. Lansberg et al., Single-Transverse-Spin-Asymmetry studies with a fixed-target experiment using the LHC beams (AFTER@LHC), PoS **DIS2016**, 241 (2016). arXiv:1610.05228 [hep-ex]
23. J.-P. Lansberg et al., Physics case for a polarised target for AFTER@LHC, PoS **PSTP2015**, 042 (2016). arXiv:1602.06857 [nucl-ex]
24. A. Signori, Gluon TMDs in quarkonium production. Few Body Syst. **57**(8), 651–655 (2016). arXiv:1602.03405 [hep-ph]
25. C. Pisano, Momentum imbalance observables as a probe of gluon TMDs, PoS **QCDEV2015**, 024 (2015). arXiv:1512.08143 [hep-ph]
26. R. Vogt, Gluon shadowing effects on J/ψ and Υ production in p + Pb Collisions at $\sqrt{s_{NN}}$= 115 GeV and p + Pb collisions at $\sqrt{s_{NN}}$= 72 GeV at AFTER@LHC. Adv. High Energy Phys. **2015**, 492302 (2015). arXiv:1510.03976 [hep-ph]
27. Y. Feng, J.-X. Wang, Next-to-leading order differential cross sections for, and production in proton–proton collisions at a fixed-target experiment using the LHC beams. Adv. High Energy Phys. **2015**, 726393 (2015). arXiv:1510.05277 [hep-ph]
28. C. Barschel, P. Lenisa, A. Nass, E. Steffens, A gas target internal to the LHC for the study of pp single-spin asymmetries and heavy ion collisions. Adv. High Energy Phys. **2015**, 463141 (2015)
29. D. Kikola, Prospects for open heavy flavor measurements in heavy ion and p + a collisions in a fixed-target experiment at the LHC. Adv. High Energy Phys. **2015**, 783134 (2015)
30. A.B. Kurepin, N.S. Topilskaya, Quarkonium production and proposal of the new experiments on fixed target at the LHC. Adv. High Energy Phys. **2015**, 760840 (2015)
31. K. Zhou, Z. Chen, P. Zhuang, Antishadowing effect on charmonium production at a fixed-target experiment using LHC beams. Adv. High Energy Phys. **2015**, 439689 (2015). arXiv:1507.05413 [nucl-th]
32. F. Arleo, S. Peigné, Quarkonium suppression from coherent energy loss in fixed-target experiments using LHC beams. Adv. High Energy Phys. **2015**, 961951 (2015). arXiv:1504.07428 [hep-ph]
33. J.-P. Lansberg, H.-S. Shao, Double-quarkonium production at a fixed-target experiment at the LHC (AFTER@LHC). Nucl. Phys. B **900**, 273–294 (2015). arXiv:1504.06531 [hep-ph]
34. S.J. Brodsky, A. Kusina, F. Lyonnet, I. Schienbein, H. Spiesberger, R. Vogt, A review of the intrinsic heavy quark content of the nucleon. Adv. High Energy Phys. **2015**, 231547 (2015). arXiv:1504.06287 [hep-ph]
35. L. Massacrier, B. Trzeciak, F. Fleuret, C. Hadjidakis, D. Kikola, J.P. Lansberg, H.S. Shao, Feasibility studies for quarkonium production at a fixed-target experiment using the LHC proton and lead beams (AFTER@LHC). Adv. High Energy Phys. **2015**, 986348 (2015). arXiv:1504.05145 [hep-ex]
36. M. Anselmino, U. D'Alesio, S. Melis, Transverse single-spin asymmetries in proton–proton collisions at the AFTER@LHC experiment in a TMD factorisation scheme. Adv. High Energy Phys. **2015**, 475040 (2015). arXiv:1504.03791 [hep-ph]
37. J.P. Lansberg, L. Szymanowski, J. Wagner, Lepton-pair production in ultraperipheral collisions at AFTER@LHC. JHEP **09**, 087 (2015). arXiv:1504.02733 [hep-ph]
38. F.A. Ceccopieri, Studies of backward particle production with a fixed-target experiment using the LHC beams. Adv. High Energy Phys. **2015**, 652062 (2015). arXiv:1503.05813 [hep-ph]
39. V.P. Goncalves, W.K. Sauter, η_c production in photon-induced interactions at a fixed target experiment at LHC as a probe of the odderon. Phys. Rev. D **91**(9), 094014 (2015). arXiv:1503.05112 [hep-ph]
40. K. Kanazawa, Y. Koike, A. Metz, D. Pitonyak, Transverse single-spin asymmetries in proton-proton collisions at the AFTER@LHC experiment. Adv. High Energy Phys. **2015**, 257934 (2015). arXiv:1502.04021 [hep-ph]
41. J.P. Lansberg, Back-to-back isolated photon-quarkonium production at the LHC and the transverse-momentum-dependent distributions of the gluons in the proton. Int. J. Mod. Phys. Conf. Ser. **40**, 1660015 (2016). arXiv:1502.02263 [hep-ph]
42. L. Massacrier et al., Studies of transverse-momentum-dependent distributions with a fixed-target experiment using the LHC beams (AFTER@LHC). Int. J. Mod. Phys. Conf. Ser. **40**(01), 1660107 (2016). arXiv:1502.00984 [nucl-ex]
43. J.P. Lansberg et al., Spin physics and TMD studies at A Fixed-Target ExpeRiment at the LHC (AFTER@LHC). EPJ Web Conf. **85**, 02038 (2015). arXiv:1410.1962 [hep-ex]
44. G. Chen, X.-G. Wu, J.-W. Zhang, H.-Y. Han, H.-B. Fu, Hadronic production of Ξ_{cc} at a fixed-target experiment at the LHC. Phys. Rev. D **89**(7), 074020 (2014). arXiv:1401.6269 [hep-ph]
45. A. Rakotozafindrabe et al., Spin physics at a fixed-target experiment at the LHC (AFTER@LHC). Phys. Part. Nucl. **45**, 336–337 (2014). arXiv:1301.5739 [hep-ex]
46. J.P. Lansberg et al., AFTER@LHC: a precision machine to study the interface between particle and nuclear physics. EPJ Web Conf. **66**, 11023 (2014). arXiv:1308.5806 [hep-ex]
47. J. P. Lansberg et al., Prospects for a fixed-target experiment at the LHC: AFTER@LHC, PoS **ICHEP2012**, 547 (2013). arXiv:1212.3450 [hep-ex]
48. C. Lorce et al., Spin and diffractive physics with a Fixed-Target ExpeRiment at the LHC (AFTER@LHC). arXiv:1212.0425 [hep-ex]. [AIP Conf. Proc.1523,149(2012)]
49. A. Rakotozafindrabe et al., Ultra-relativistic heavy-ion physics with AFTER@LHC. Nucl. Phys. **A904–905**, 957c–960c (2013). arXiv:1211.1294 [nucl-ex]
50. J. P. Lansberg et al., A Fixed-Target ExpeRiment at the LHC (AFTER@LHC) : luminosities, target polarisation and a selection of physics studies, Po**SQNP2012**, 049 (2012). arXiv:1207.3507 [hep-ex]
51. J.P. Lansberg, S.J. Brodsky, F. Fleuret, C. Hadjidakis, Quarkonium physics at a fixed-target experiment using the LHC beams. Few Body Syst. **53**, 11–25 (2012). arXiv:1204.5793 [hep-ph]

52. T. Liu, B.-Q. Ma, Azimuthal asymmetries in lepton-pair production at a fixed-target experiment using the LHC beams (AFTER). Eur. Phys. J. C **72**, 2037 (2012). arXiv:1203.5579 [hep-ph]
53. E. Steffens, Estimation of the performance of a HERMES type gas target internal to the LHC. PoS **PSTP2015**, 019 (2015)
54. D.W. Sivers, Single spin production asymmetries from the hard scattering of point-like constituents. Phys. Rev. D **41**, 83 (1990)
55. S.J. Brodsky, D.S. Hwang, I. Schmidt, Initial state interactions and single spin asymmetries in Drell–Yan processes. Nucl. Phys. **B642**, 344–356 (2002). arXiv:hep-ph/0206259 [hep-ph]
56. U. D'Alesio, F. Murgia, Azimuthal and single spin asymmetries in hard scattering processes. Prog. Part. Nucl. Phys. **61**, 394–454 (2008). arXiv:0712.4328 [hep-ph]
57. V. Barone, F. Bradamante, A. Martin, Transverse-spin and transverse-momentum effects in high-energy processes. Prog. Part. Nucl. Phys. **65**, 267–333 (2010). arXiv:1011.0909 [hep-ph]
58. R. Angeles-Martinez et al., Transverse momentum dependent (TMD) parton distribution functions: status and prospects. Acta Phys. Polon. B **46**(12), 2501–2534 (2015). arXiv:1507.05267 [hep-ph]
59. C. Kouvaris, J.-W. Qiu, W. Vogelsang, F. Yuan, Single transverse-spin asymmetry in high transverse momentum pion production in pp collisions. Phys. Rev. D **74**, 114013 (2006). arXiv:hep-ph/0609238 [hep-ph]
60. B.E. Bonner et al., Analyzing power measurement in inclusive pi0 production at high x(f). Phys. Rev. Lett. **61**, 1918 (1988)
61. E704, E581 Collaboration, D. L. Adams et al., Comparison of spin asymmetries and cross sections in π^0 production by 200 GeV polarized anti-protons and protons, Phys. Lett. **B261**, 201–206 (1991)
62. PHENIX Collaboration, A. Adare et al., Measurement of transverse-single-spin asymmetries for midrapidity and forward-rapidity production of hadrons in polarized p+p collisions at $\sqrt{s}$ =200 and 62.4 GeV, *Phys. Rev.***D90**(1), 012006 (2014). arXiv:1312.1995 [hep-ex]
63. A. Lesnik, D.M. Schwartz, I. Ambats, E. Hayes, W.T. Meyer, C.E.W. Ward, T.M. Knasel, E.C. Swallow, R. Winston, T.A. Romanowski, Observation of a difference between polarization and analyzing power in Lambda0 production with 6-GeV/c polarized protons. Phys. Rev. Lett. **35**, 770 (1975)
64. G. Bunce et al., Λ^0 hyperon polarization in inclusive production by 300 GeV protons on beryllium. Phys. Rev. Lett. **36**, 1113–1116 (1976)
65. FNAL-E704 Collaboration, D. L. Adams et al., Analyzing power in inclusive π^+ and π^- production at high x(F) with a 200 GeV polarized proton beam, Phys. Lett. **B264**, 462–466 (1991)
66. E704, E581 Collaboration, D. L. Adams et al., Large x(F) spin asymmetry in π^0 production by 200 GeV polarized protons, Z. Phys. **C56**, 181–184 (1992)
67. K. Krueger et al., Large analyzing power in inclusive $\pi^\pm$ production at high x(F) with a 22 GeV/c polarized proton beam. Phys. Lett. B **459**, 412–416 (1999)
68. V. Barone, P.G. Ratcliffe, *Transverse Spin Physics* (World Scientific, River Edge, 2003)
69. E. Leader, Spin in particle physics. Camb. Monogr. Part. Phys. Nucl. Phys. Cosmol. **15**, 1–500 (2011)
70. F. Pijlman, Single Spin Asymmetries and Gauge Invariance in Hard Scattering Processes. Ph.D. thesis, Vrije U., Amsterdam, 2006. arXiv:hep-ph/0604226 [hep-ph]. http://www.nikhef.nl/pub/services/biblio/theses_pdf/thesis_F_Pijlman.pdf
71. C. J. Bomhof, Azimuthal Spin Asymmetries in Hadronic Processes. Ph.D. thesis, Vrije U., Amsterdam, 2007. http://inspirehep.net/record/761943/files/8060.pdf
72. V. Barone, A. Drago, P.G. Ratcliffe, Transverse polarisation of quarks in hadrons. Phys. Rept. **359**, 1–168 (2002). arXiv:hep-ph/0104283 [hep-ph]
73. C. Bourrely, J. Soffer, E. Leader, Polarization phenomena in hadronic reactions. Phys. Rept. **59**, 95–297 (1980)
74. M. Anselmino, A. Efremov, E. Leader, The theory and phenomenology of polarized deep inelastic scattering. Phys. Rept.**261**, 1–124 (1995). arXiv:hep-ph/9501369 [hep-ph]. [Erratum: Phys. Rept.281,399(1997)]
75. Z.-T. Liang, C. Boros, Single spin asymmetries in inclusive high-energy hadron hadron collision processes. Int. J. Mod. Phys. A **15**, 927–982 (2000). arXiv:hep-ph/0001330 [hep-ph]
76. M. Boglione, A. Prokudin, Phenomenology of transverse spin: past, present and future. Eur. Phys. J. A **52**(6), 154 (2016). arXiv:1511.06924 [hep-ph]
77. E.C. Aschenauer, U. D'Alesio, F. Murgia, TMDs and SSAs in hadronic interactions. Eur. Phys. J. A **52**(6), 156 (2016). arXiv:1512.05379 [hep-ph]
78. A. Prokudin, A_N in inclusive lepton-proton collisions: TMD and twist-3 approaches. EPJ Web Conf. **85**, 02028 (2015). arXiv:1410.3867 [hep-ph]
79. A.V. Efremov, O.V. Teryaev, On spin effects in quantum chromodynamics. Sov. J. Nucl. Phys. **36**, 140 (1982). [Yad. Fiz.36,242(1982)]
80. J.-W. Qiu, G.F. Sterman, Single transverse spin asymmetries. Phys. Rev. Lett. **67**, 2264–2267 (1991)
81. D.W. Sivers, Hard scattering scaling laws for single spin production asymmetries. Phys. Rev. D **43**, 261–263 (1991)
82. J. Collins, *Foundations of perturbative QCD*. (Cambridge University Press, 2013). http://www.cambridge.org/de/knowledge/isbn/item5756723
83. M.G. Echevarria, A. Idilbi, I. Scimemi, Factorization theorem for Drell-Yan at low q_T and transverse momentum distributions on-the-light-cone. JHEP **07**, 002 (2012). arXiv:1111.4996 [hep-ph]
84. M.G. Echevarria, A. Idilbi, I. Scimemi, Soft and collinear factorization and transverse momentum dependent parton distribution functions. Phys. Lett. B **726**, 795–801 (2013). arXiv:1211.1947 [hep-ph]
85. M.G. Echevarria, A. Idilbi, I. Scimemi, Unified treatment of the QCD evolution of all (un-)polarized transverse momentum dependent functions: collins function as a study case. Phys. Rev. D **90**(1), 014003 (2014). arXiv:1402.0869 [hep-ph]
86. M.G. Echevarria, T. Kasemets, P.J. Mulders, C. Pisano, QCD evolution of (un)polarized gluon TMDPDFs and the Higgs q_T-distribution. JHEP **07**, 158 (2015). arXiv:1502.05354 [hep-ph]
87. U. D'Alesio, F. Murgia, Parton intrinsic motion in inclusive particle production: unpolarized cross sections, single spin asymmetries and the Sivers effect. Phys. Rev. D **70**, 074009 (2004). arXiv:hep-ph/0408092 [hep-ph]
88. M. Anselmino, M. Boglione, U. D'Alesio, E. Leader, F. Murgia, Parton intrinsic motion: suppression of the Collins mechanism for transverse single spin asymmetries in p(up) p −> pi X. Phys. Rev. D **71**, 014002 (2005). arXiv:hep-ph/0408356 [hep-ph]

89. D. Boer, P.J. Mulders, F. Pijlman, Universality of T odd effects in single spin and azimuthal asymmetries. Nucl. Phys. B **667**, 201–241 (2003). arXiv:hep-ph/0303034 [hep-ph]
90. COMPASS Collaboration, C. Quintans, Future Drell-Yan measurements in COMPASS. J. Phys. Conf. Ser. **295**, 012163 (2011)
91. A. Klein, X. Jiang, D. Gessaman, P. Reimer, C. Brown, F. Christian, M. Diefenthaler, J.-C. Peng, W.-C. Chang, Y.-C. Chen et al., Letter of Intent for a Drell-Yan experiment with a polarized proton target, FERMILAB-LOI-2013-01. http://inspirehep.net/record/1240849
92. L.D. Isenhower, T. Hague, R. Towell, S. Watson, C. Aidala, C. Dutta, W. Lorenzon, R. Raymond, Z. Qu, J. Arrington et al, Polarized Drell-Yan measurements with the Fermilab Main Injector, FERMILAB-PROPOSAL-1027. http://inspirehep.net/record/1216817?ln=en
93. J.-W. Qiu, G.F. Sterman, Single transverse spin asymmetries in direct photon production. Nucl. Phys. B **378**, 52–78 (1992)
94. M.G.A. Buffing, A. Mukherjee, P.J. Mulders, Generalized universality of definite rank gluon transverse momentum dependent correlators. Phys. Rev. D **88**, 054027 (2013). arXiv:1306.5897 [hep-ph]
95. D. Boer, C. Lorce, C. Pisano, J. Zhou, The gluon Sivers distribution: status and future prospects. Adv. High Energy Phys. **2015**, 371396 (2015). arXiv:1504.04332 [hep-ph]
96. C. Pisano, D. Boer, S.J. Brodsky, M.G.A. Buffing, P.J. Mulders, Linear polarization of gluons and photons in unpolarized collider experiments. JHEP **10**, 024 (2013). arXiv:1307.3417 [hep-ph]
97. D. Boer, W.J. den Dunnen, TMD evolution and the Higgs transverse momentum distribution. Nucl. Phys. B **886**, 421–435 (2014). arXiv:1404.6753 [hep-ph]
98. LHCb Collaboration, R. Aaij et al., Measurement of the $\eta_c(1S)$ production cross-section in proton–proton collisions via the decay $\eta_c(1S) \to p\bar{p}$, Eur. Phys. J. **C75**(7), 311 (2015). arXiv:1409.3612 [hep-ex]
99. LHCb Collaboration, R. Aaij et al., Observation of $\eta_c(2S) \to p\bar{p}$ and search for $X(3872) \to p\bar{p}$ decays. arXiv:1607.06446 [hep-ex]
100. LHCb Collaboration, R. Aaij et al., Measurement of the ratio of prompt χ_c to J/ψ production in pp collisions at $\sqrt{s} = 7$ TeV. Phys. Lett.**B718**, 431–440 (2012). arXiv:1204.1462 [hep-ex]
101. LHCb Collaboration, R. Aaij et al., Measurement of the cross-section ratio $\sigma(\chi_{c2})/\sigma(\chi_{c1})$ for prompt χ_c production at $\sqrt{s} = 7$ TeV. Phys. Lett.**B714**, 215–223 (2012). arXiv:1202.1080 [hep-ex]
102. Z.-B. Kang, J.-W. Qiu, W. Vogelsang, F. Yuan, Accessing tri-gluon correlations in the nucleon via the single spin asymmetry in open charm production. Phys. Rev. D **78**, 114013 (2008). arXiv:0810.3333 [hep-ph]
103. X.-D. Ji, Gluon correlations in the transversely polarized nucleon. Phys. Lett. B **289**, 137–142 (1992)
104. H. Beppu, Y. Koike, K. Tanaka, S. Yoshida, Contribution of twist-3 multi-gluon correlation functions to single spin asymmetry in semi-inclusive deep inelastic scattering. Phys. Rev. D **82**, 054005 (2010). arXiv:1007.2034 [hep-ph]
105. W.J. den Dunnen, J.P. Lansberg, C. Pisano, M. Schlegel, Accessing the transverse dynamics and polarization of gluons inside the proton at the LHC. Phys. Rev. Lett. **112**, 212001 (2014). arXiv:1401.7611 [hep-ph]
106. LHCb Collaboration, A. A. Alves, Jr. et al., The LHCb Detector at the LHC, JINST **3**, S08005 (2008)
107. ALICE Collaboration, K. Aamodt et al., The ALICE experiment at the CERN LHC. JINST**3**, S08002 (2008)
108. LHCb Collaboration, R. Aaij et al., Precision luminosity measurements at LHCb. JINST **9**(12), P12005 (2014). arXiv:1410.0149 [hep-ex]
109. Technical Design Report for the Muon Forward Tracker, Tech. Rep. CERN-LHCC-2015-001. ALICE-TDR-018, Jan, 2015. https://cds.cern.ch/record/1981898
110. ALICE Collaboration, J. Adam et al., Inclusive quarkonium production at forward rapidity in pp collisions at $\sqrt{s} = 8$ TeV. Eur. Phys. J. **C76**(4), 184 (2016). arXiv:1509.08258 [hep-ex]
111. NA60 Collaboration, R. Arnaldi et al., Evidence for the production of thermal-like muon pairs with masses above 1-GeV/c**2 in 158-A-GeV Indium–Indium Collisions. Eur. Phys. J. **C59**, 607–623 (2009). arXiv:0810.3204 [nucl-ex]
112. J.-W. Qiu, M. Schlegel, W. Vogelsang, Probing gluonic spin-orbit correlations in photon pair production. Phys. Rev. Lett. **107**, 062001 (2011). arXiv:1103.3861 [hep-ph]
113. D. Boer, C. Pisano, Impact of gluon polarization on Higgs boson plus jet production at the LHC. Phys. Rev. D **91**(7), 074024 (2015). arXiv:1412.5556 [hep-ph]
114. M.G. Echevarria, A. Idilbi, A. Schaefer, I. Scimemi, Model-independent evolution of transverse momentum dependent distribution functions (TMDs) at NNLL. Eur. Phys. J. C **73**(12), 2636 (2013). arXiv:1208.1281 [hep-ph]
115. E. Steffens, W. Haeberli, Polarized gas targets. Rep. Progress Phys. **66**(11), 1887 (2003). http://stacks.iop.org/0034-4885/66/i=11/a=R02
116. R. G. Milner. Private communication
117. CMS, TOTEM Collaboration, S. Chatrchyan et al., Measurement of pseudorapidity distributions of charged particles in proton-proton collisions at $\sqrt{s}$ = 8 TeV by the CMS and TOTEM experiments. Eur. Phys. J. **C74**(10), 3053 (2014). arXiv:1405.0722 [hep-ex]